 CMES, vol.9, no.2, pp.133-150, 2005

Finite Element Approaches to Non-classical Heat Conduction in Solids

S. Bargmann and P. Steinmann[1]

Abstract: The present contribution is concerned with the modeling and computation of non-classical heat conduction. In the 90s Green and Naghdi presented a new theory which is fully consistent. We suggest a solution method based on finite elements for the spatial as well as for the temporal discretization. A numerical example is compared to existing experimental results in order to illustrate the performance of the method.

keyword: Galerkin finite elements, heat conduction, second sound

1 Introduction

Motivated by experiments hyperbolic theories of thermoelasticity which lead to a wave-type heat conduction were developed in recent years. This paper deals with the thermal aspect following the approach suggested by Green and Naghdi in [Green and Naghdi (1991, 1992, 1993)].

In 1946 Peshkov was the first to propose the possibility of heat propagation as thermal waves in solids [Peshkov (1946)] after having detected this phenomenon in fluid helium II in 1944 [Peshkov (1944)]. The existence of the so called second sound in solids was proven in 1966 by Ackermann, Bertram, Fairbank, and Gyuer (1966) for solid He^4. So far second sound was also detected in solid He^3 and in the dielectric crystals of NaF and Bi. It can only be observed in a small range at low temperatures.

The theory of Green and Naghdi is rather unusual as it relies on a general entropy balance instead of an entropy inequality. Besides that they introduce a new quantity

$$\alpha = \int_{t_0}^{t} T\left(\boldsymbol{x}, \tau\right) \mathrm{d}\tau + \alpha_0, \tag{1}$$

with T and $\boldsymbol{x}$ being the empirical temperature and the spatial coordinates, resp.. α is called the thermal displacement. Green and Naghdi's non-classical theory is based on three different constitutive equations for the heat flux, labeled type I, II and III. The linearized theory I corresponds to Fourier's law, consequently, the classical theory is fully embedded. Type II entails a hyperbolic heat equation which allows the transmission of heat as thermal waves without energy dissipation. One of the obvious errors of the diffusion equation is the paradox of infinite wave propagation speed. Both, type II and III (being an extension of II which involves energy dissipation), allow heat transmission at finite speed and therefore are likely to be more naturally suitable than the usual theory of Fourier.

Several results on different theoretical aspects of the theory of Green and Naghdi have been published. Chandrasekharaiah (1996a,b) worked on the uniqueness, Nappa (1998) on spatial behavior in the linear theory. Iesan (1998) focused on type II. Quintanilla and Straughan published a number of papers, e.g. on stability [Quintanilla (2001b)] and instability [Quintanilla (2001a,b)] of solutions, existence [Quintanilla (2002)] or acceleration waves [Quintanilla and Straughan (2004)]. Maugin and Kalpakides addressed themselves to the Lagrangian and the Hamiltonian formulation [Maugin and Kalpadikes (2002a,b)] of Green and Naghdi's theory. Only a handful of papers appeared using aspects of the theory of Green and Naghdi for numerical modeling, see e.g. Misra, Chattopadhyay, and Chakravorty (2000), Puri and Jordan (2004) or Allam, Elsibai, and AbouElregal (2002). As far as we know there exist no publications concerning the computational modeling of original second sound heat pulse experiments with the Green-Naghdi approach.

The aim of our contribution is the numerical treatment of Green and Naghdi's theory. It is structured as follows. First we reiterate the basic ideas and equations of Green and Naghdi (1991). Section 3 focuses on spatial and temporal discretization. Then the linear theory of heat conduction for isotropic and homogeneous materials is applied to a rigid conductor in a range of low tempera-

[1] Chair of Applied Mechanics, Department of Mechanical Engineering, University of Kaiserslautern, Germany

tures where heat pulses appear due to a sudden change in temperature. Finally the results are compared to given experimental data.

2 Theory of Heat Conduction in Solids

During the second half of the last century there has been reasonable interest in the theory of heat conduction in solids. The detection of second sound and the unnatural property of Fourier's law that heat waves may propagate with infinite speed entailed several considerations. Nevertheless the problem of an exact theoretical model has not yet been solved. In [Green and Naghdi (1991)] Green and Naghdi introduce a theory which attracted interest as heat propagates as thermal waves at finite speed and does not necessarily involve energy dissipation. Another recent non-classical model was developed by Kosinski, Cimmmelli and Frischmuth [Cimmelli and Kosiński (1991); Frischmuth and Cimmelli (1996)] by defining an internal state variable called semi-empirical temperature. Chandrasekharaiah (1998) and Tzou (1995) modify Fourier's law with two different time translations for the temperature gradient as well as for the heat flux which leads to a dual-phase-lag thermoelasticity. Hetnarski and Ignaczak (1996) use an energy function and a heat flux which both depend on an elastic heat flow in addition to the temperature and the strain tensor.

Only some of the latest ideas are mentioned above as there exist excellent and very detailed overviews of the development, which was done by reviewing a great number of publications, in Joseph and Preziosi (1989, 1990) and in Tamma and Namburu (1997). The focus of this paper is the Green-Naghdi-model which in the opinion of the authors is a very promising theory.

Heat conduction in a finite body (a stationary rigid solid) $\mathcal{B}$ is considered. We restrict ourselves to the case of an isotropic and homogeneous conductor. The position of a point x is denoted by $\boldsymbol{x}$ in the fixed configuration.

In order to measure a "mean" thermal displacement magnitude a scalar $\alpha = \alpha(\boldsymbol{x}, t)$ is defined by

$$\alpha = \int_{t_0}^{t} T(\boldsymbol{x}, \tau)\, \mathrm{d}\tau + \alpha_0, \tag{2}$$

where T represents the temperature and α_0 is the initial value of α at the reference time t_0. α is called thermal displacement and

$$\dot{\alpha} = T \tag{3}$$

holds.

Furthermore a positive scalar θ being an increasing function of T is introduced

$$\theta = \theta(T; a^*), \tag{4}$$

a^* being a set of constants.

We assume the balance of entropy stated in Green and Naghdi (1977):

$$\frac{\partial}{\partial t}\int_B \rho\eta \mathrm{d}V = \int_B \rho\,[s+\xi]\,\mathrm{d}V - \int_{\partial B} \boldsymbol{pn}\mathrm{d}A. \tag{5}$$

The corresponding local form reads

$$\rho\dot{\eta} = \rho\,[s+\xi] - \mathrm{div}\boldsymbol{p}, \tag{6}$$

where ρ is the body's density, η the entropy density per unit mass, s the external rate of entropy supply per unit mass, $\xi \geq 0$ the internal rate of entropy production per unit mass and $\boldsymbol{p}$ the entropy flux vector.

From multiplying by the scalar quantity θ we obtain

$$\rho\theta\dot{\eta} = \rho\theta\,[s+\xi] + \boldsymbol{p}\nabla\theta - \mathrm{div}\,(\theta\boldsymbol{p}). \tag{7}$$

The heat flux vector $\boldsymbol{q}$ is then related to the entropy flux vector $\boldsymbol{p}$ by the classical assumption

$$\boldsymbol{q} := \theta\boldsymbol{p}. \tag{8}$$

Thus we receive

$$\rho\theta\dot{\eta} = \rho\theta\,[s+\xi] + \boldsymbol{p}\nabla\theta - \mathrm{div}\boldsymbol{q}. \tag{9}$$

In order to develop a complete theory Green and Naghdi (1991) showed that the following energy equation is valid for all heat and thermal processes

$$\rho\dot{\psi} + \rho\dot{\theta}\eta + \boldsymbol{p}\nabla\theta + \rho\theta\xi = 0 \tag{10}$$

with ψ being the specific Helmholtz free energy.

In the following we introduce different constitutive equations for ψ, θ, η, $\boldsymbol{p}$, ξ for the three types of heat conduction.

2.1 Type I

In the case of heat flow of type I it is assumed that ψ, θ, η, $\boldsymbol{p}$, ξ are functions of the temperature T and the temperature gradient ∇T:

$$\begin{aligned} &\psi = \psi(T, \nabla T), \quad \theta = \theta(T, \nabla T), \\ &\eta = \eta(T, \nabla T), \quad \boldsymbol{p} = \boldsymbol{p}(T, \nabla T), \\ &\xi = \xi(T, \nabla T). \end{aligned} \tag{11}$$

Applying (11) to (10) yields

$$\begin{aligned} &\rho\left[\frac{\partial\psi}{\partial T}\frac{\partial T}{\partial t} + \frac{\partial\psi}{\partial\nabla T}\frac{\partial\nabla T}{\partial t}\right] + \rho\left[\frac{\partial\theta}{\partial T}\frac{\partial T}{\partial t} + \frac{\partial\theta}{\partial\nabla T}\frac{\partial\nabla T}{\partial t}\right]\eta \\ &\quad + \boldsymbol{p}\left[\frac{\partial\theta}{\partial T}\frac{\partial T}{\partial\boldsymbol{x}} + \frac{\partial\theta}{\partial\nabla T}\frac{\partial\nabla T}{\partial\boldsymbol{x}}\right] + \rho\theta\xi = 0 \end{aligned} \tag{12}$$

which again is valid for all heat and thermal processes. As a consequence it must hold for every $\dot{T}$, $\nabla\dot{T}$ and $\nabla^2 T$. Setting first all three terms equal to zero, then $\dot{T}$, $\nabla\dot{T}$ equal to zero and $\nabla^2 T$ nonzero and third $\dot{T} = 0$ and $\nabla\dot{T}$ nonzero, leads to the conclusions that $\boldsymbol{p}\nabla\theta + \rho\theta\xi = 0$ and that the Helmholtz energy ψ as well as as the positive scalar θ only depend on the temperature T and not on its gradient ∇T. Without loss of generality we set $T \equiv \theta$.

If the following relations are postulated

$$\begin{aligned} \eta &= c \ln T \\ \boldsymbol{q} &= -k\nabla T, \end{aligned} \tag{13}$$

where c and k denote, resp., the non-negative constant specific heat and the constant thermal conductivity, the entropy equation (9) reads

$$\rho c\dot{T} = \rho T s + k\Delta T. \tag{14}$$

By substituting the external rate of heat supply per unit mass $r = Ts$ the classical Fourier heat conduction results

$$\rho c\dot{T} = \rho r + k\Delta T. \tag{15}$$

2.2 Type II

The theory of type II involves heat transmission as thermal waves at finite speed without energy dissipation. Again constitutive equations are specified for ψ, θ, η, $\boldsymbol{p}$, ξ. All of them are assumed to depend on the temperature T, the thermal displacement α and the thermal displacement gradient $\nabla\alpha$:

$$\begin{aligned} &\psi = \psi(T, \alpha, \nabla\alpha), \quad \theta = \theta(T, \alpha, \nabla\alpha), \\ &\eta = \eta(T, \alpha, \nabla\alpha), \quad \boldsymbol{p} = \boldsymbol{p}(T, \alpha, \nabla\alpha), \\ &\xi = \xi(T, \alpha, \nabla\alpha). \end{aligned} \tag{16}$$

Analogously to heat flow of the Fourier type, the set of equations (16) is inserted into the energy equation (10):

$$\begin{aligned} &\rho\left[\frac{\partial\psi}{\partial T}\frac{\partial T}{\partial t} + \frac{\partial\psi}{\partial\alpha}\frac{\partial\alpha}{\partial t} + \frac{\partial\psi}{\partial\nabla T}\frac{\partial\nabla T}{\partial t}\right] \\ &+\rho\left[\frac{\partial\theta}{\partial T}\frac{\partial T}{\partial t} + \frac{\partial\theta}{\partial\alpha}\frac{\partial\alpha}{\partial t} + \frac{\partial\theta}{\partial\nabla T}\frac{\partial\nabla T}{\partial t}\right]\eta \\ &+\boldsymbol{p}\left[\frac{\partial\theta}{\partial T}\frac{\partial T}{\partial\boldsymbol{x}} + \frac{\partial\theta}{\partial\alpha}\frac{\partial\alpha}{\partial\boldsymbol{x}} + \frac{\partial\theta}{\partial\nabla T}\frac{\partial\nabla T}{\partial\boldsymbol{x}}\right] + \rho\theta\xi = 0. \end{aligned} \tag{17}$$

Green and Naghdi (1991) proved θ must be independent of the thermal displacement gradient $\nabla\alpha$ and suggest the following linearized assumptions:

$$\begin{aligned} \theta &= a + bT \\ \boldsymbol{p} &= \frac{1}{\theta}\boldsymbol{q} = -\frac{\rho k}{b}\nabla\alpha \\ \eta &= c\ln\theta \\ \xi &= 0 \end{aligned} \tag{18}$$

where a and b denote positive constants.

Consequently the entropy equation (9) results in

$$\rho c b\dot{T} = \rho r + \rho\frac{a}{b}k\Delta\alpha, \tag{19}$$

neglecting the nonlinear terms.

In the case of a constant external rate of heat supply per unit mass ($\dot{r} = 0$) and a positive thermal conductivity ($k > 0$) the time derivative of (19) is the well-known standard wave equation

$$\ddot{T} = \frac{ak}{cb^2}\Delta T, \tag{20}$$

which represents waves propagating undamped with a speed of

$$v = \sqrt{\frac{ak}{cb^2}}. \tag{21}$$

Note that Green and Naghdi (1991) deduce the entropy flux vector $\boldsymbol{p}$ from a potential in the same way the stress tensor is derived in mechanics:

$$\boldsymbol{p} = -\frac{\rho}{\frac{\partial\theta}{\partial T}}\frac{\partial\psi}{\partial\nabla\alpha} = -\frac{\rho k}{b}\nabla\alpha \tag{22}$$

as $\psi = c\left[\theta - \theta \ln \theta\right] + \frac{1}{2} k \nabla\alpha\nabla\alpha$.

2.3 Type III

In case of heat flow of type III a dependency of ψ, θ, η, $\boldsymbol{p}$, ξ on the temperature T, the thermal displacement α and their gradients ∇T and $\nabla\alpha$ is assumed:

$$\begin{aligned}
\psi &= \psi\left(T, \alpha, \nabla T, \nabla\alpha\right), \quad \theta = \theta\left(T, \alpha, \nabla T, \nabla\alpha\right), \\
\eta &= \eta\left(T, \alpha, \nabla T, \nabla\alpha\right), \quad \boldsymbol{p} = \boldsymbol{p}\left(T, \alpha, \nabla T, \nabla\alpha\right), \\
\xi &= \xi\left(T, \alpha, \nabla T, \nabla\alpha\right).
\end{aligned} \tag{23}$$

As in the previous two approaches the constitutive relations (23) are substituted into the energy equation (10) and the following relations are concluded in Green and Naghdi (1991) :

$$\begin{aligned}
\theta &= a + bT + d\alpha \\
\boldsymbol{q} &= \theta\boldsymbol{p} = -k_1\nabla\alpha + k_2\nabla T \\
\eta &= \frac{b_2\alpha + b_3 T}{b} \\
\xi &= 0.
\end{aligned} \tag{24}$$

a, b, b_2, b_3, d are positive constants. The temperature equation for the third heat flow is found by inserting (24) into the entropy equation (9) and retaining only linear terms

$$\rho\frac{a}{b}\left[b_2\dot{\alpha} + b_3\dot{T}\right] = \rho r + k_1\Delta\alpha + k_2\Delta T. \tag{25}$$

3 Finite Element Discretization

In this section we provide detailed information about the finite element discretization we use. We apply a discretization method, using a standard Bubnov-Galerkin finite element method in space and a Galerkin finite element formulation in time.

3.1 Spatial

To construct the weak form the temperature equations (15), (19) and (25) are weighted with a test function δT and integrated over the domain $\mathcal{B}$. After applying the divergence theorem we obtain in case of type I

$$\begin{aligned}
&\int_{\mathcal{B}} \delta T \rho c \dot{T} \,\mathrm{d}V + \int_{\mathcal{B}} \nabla\delta T k \nabla T \,\mathrm{d}V \\
&= \int_{\mathcal{B}} \delta T \rho r \,\mathrm{d}V - \int_{\partial\mathcal{B}} \delta T k \nabla T \boldsymbol{n} \,\mathrm{d}A
\end{aligned} \tag{26}$$

or for type II

$$\begin{aligned}
&\int_{\mathcal{B}} \delta T \rho c b \dot{T} \,\mathrm{d}V + \int_{\mathcal{B}} \nabla\delta T \rho\frac{a}{b} k \nabla\alpha \,\mathrm{d}V \\
&= \int_{\mathcal{B}} \delta T \rho r \,\mathrm{d}V - \int_{\partial\mathcal{B}} \delta T \rho\frac{a}{b} k \nabla\alpha \boldsymbol{n} \,\mathrm{d}A
\end{aligned} \tag{27}$$

or for type III

$$\begin{aligned}
&\int_{\mathcal{B}} \delta T \rho\frac{a}{b}\left[b_2\dot{\alpha} + b_3\dot{T}\right] \mathrm{d}V + \int_{\mathcal{B}} \nabla\delta T \left[k_1\nabla\alpha + k_2\nabla T\right] \mathrm{d}V \\
&\qquad = \int_{\mathcal{B}} \delta T \rho r \,\mathrm{d}V - \int_{\partial\mathcal{B}} \delta T \left[k_1\nabla\alpha + k_2\nabla T\right] \boldsymbol{n} \,\mathrm{d}A
\end{aligned} \tag{28}$$

The domain $\mathcal{B}$ is discretized into n_{el} spatial elements and the geometry $\boldsymbol{x}$ is interpolated elementwise by shape functions N^i at the $i = 1, \ldots, n_{en}$ node point positions.

$$\mathcal{B} = \bigcup_{e=1}^{n_{el}} \mathcal{B}^e \qquad \boldsymbol{x}^h\,|_{\mathcal{B}^e} = \sum_{i=1}^{n_{en}} N^i \boldsymbol{x}_i \tag{29}$$

Following the isoparametric concept we interpolate the unknowns, the temperature T and the thermal displacement α, with the same shape functions N^i as the element geometry $\boldsymbol{x}$. Furthermore, according to the Bubnov-Galerkin method, the test function δT is discretized with these test functions N^i, too.

$$\begin{aligned}
\alpha^h|_{\mathcal{B}^e} &= \sum_{i=1}^{n_{en}} N^i \alpha_i \\
T^h|_{\mathcal{B}^e} &= \sum_{i=1}^{n_{en}} N^i T_i \\
\delta T^h|_{\mathcal{B}^e} &= \sum_{i=1}^{n_{en}} N^i \delta T_i
\end{aligned} \tag{30}$$

Thus we receive the following expressions for the discrete gradients of the unknowns $\nabla\alpha$, ∇T and of the test function $\nabla\delta T$:

$$\begin{aligned}
\nabla\alpha^h|_{\mathcal{B}^e} &= \sum_{i=1}^{n_{en}} \alpha_i \nabla N^i \\
\nabla T^h|_{\mathcal{B}^e} &= \sum_{i=1}^{n_{en}} T_i \nabla N^i \\
\nabla\delta T^h|_{\mathcal{B}^e} &= \sum_{i=1}^{n_{en}} \delta T_i \nabla N^i.
\end{aligned} \tag{31}$$

Consequently, we obtain the following semi-discretized temperature equations for type I-III:

$$\boldsymbol{C}_{\rho c} \cdot \dot{\boldsymbol{T}}\left(t\right) + \boldsymbol{K}_k \cdot \boldsymbol{T}\left(t\right) = \boldsymbol{F}_{\text{source}} - \boldsymbol{F}_I \tag{32}$$

$$\boldsymbol{C}_{\rho cb} \cdot \dot{\boldsymbol{T}}(t) + \boldsymbol{K}_{\rho \frac{a}{b} k} \cdot \boldsymbol{\alpha}(t) = \boldsymbol{F}_{\text{source}} - \boldsymbol{F}_{II} \tag{33}$$

$$\boldsymbol{C}_{\rho \frac{a}{b} b_2} \cdot \dot{\boldsymbol{\alpha}}(t) + \boldsymbol{C}_{\rho \frac{a}{b} b_3} \cdot \dot{\boldsymbol{T}}(t) + \boldsymbol{K}_{k_1} \cdot \boldsymbol{\alpha}(t) + \boldsymbol{K}_{k_2} \cdot \boldsymbol{T}(t) = \boldsymbol{F}_{\text{source}} - \boldsymbol{F}_{III} \tag{34}$$

The capacity matrices are of the format:

$$\boldsymbol{C}_{\bullet} = \mathop{\boldsymbol{A}}_{e=1}^{n_{el}} \int_{\mathcal{B}^e} N^i \bullet N^j \mathrm{d}V$$

in the sense that e.g.

$$\boldsymbol{C}_{\rho c} := \mathop{\boldsymbol{A}}_{e=1}^{n_{el}} \int_{\mathcal{B}^e} N^i \rho c N^j \mathrm{d}V \tag{35}$$

The conductance matrices are expressed as

$$\boldsymbol{K}_{\bullet} = \mathop{\boldsymbol{A}}_{e=1}^{n_{el}} \int_{\mathcal{B}^e} \nabla N^i \bullet \nabla N^j \mathrm{d}V.$$

On the right-hand side the heat load vector due to external heat bulk source

$$\boldsymbol{F}_{\text{source}} = \mathop{\boldsymbol{A}}_{e=1}^{n_{el}} \int_{\mathcal{B}^e} N^i \rho r \mathrm{d}V$$

and those due to specified nodal temperatures

$$\boldsymbol{F}_{I} = \mathop{\boldsymbol{A}}_{e=1}^{n_{el}} \int_{\partial \mathcal{B}^e} N^i k \nabla T \boldsymbol{n} \mathrm{d}A \quad \boldsymbol{F}_{II} = \mathop{\boldsymbol{A}}_{e=1}^{n_{el}} \int_{\partial \mathcal{B}^e} N^i \rho \frac{a}{b} k \nabla \alpha \boldsymbol{n} \mathrm{d}A$$

$$\boldsymbol{F}_{III} = \mathop{\boldsymbol{A}}_{e=1}^{n_{el}} \int_{\partial \mathcal{B}^e} N^i \left[k_1 \nabla \alpha + k_2 \nabla T \right] \boldsymbol{n} \mathrm{d}A$$

are obtained.

The operator $\mathop{\boldsymbol{A}}_{e=1}^{n_{el}}$ denotes the assembly over all element contributions at the element nodes.

3.2 Temporal

Each of the temperature equations (15), (19) and (25) has to be discretized in time as well. In order to perpetuate the consistency of the theory to the numerical aspect we resort to a Galerkin finite element method in time as well. At this point we distinguish between the discontinuous Galerkin (dG) method and the continuous Galerkin (cG) method. The former one is ascribed to Lasaint and Raviart (1974) while the latter one is acclaimed to Hulme (1972).

For deeper studies of both methods see e.g. Eriksson, Estep, Hansbo, and Johnson (1996). Betsch and Steinmann have published several papers [Betsch and Steinmann (2000a,b, 2001)] on the energy conserving properties of the cG method in elastodynamics.

3.2.1 Discontinuous Galerkin Method

Retaining the terminology of Eriksson in Eriksson, Estep, Hansbo, and Johnson (1996) the expression "dG(k) method" signifies that the trial as well as the test functions are of discontinuous piecewise polynomials of degree k. The identical function spaces are an advantage in the error analysis and gain improved stability properties for parabolic problems [Eriksson, Estep, Hansbo, and Johnson (1996)].

The time interval of interest $I = [t_0, t_0 + t_T]$ is divided into a finite number n_t of elements such that

$$\int_{t_0}^{t_0+t_T} [\ldots] \mathrm{d}t = \sum_{i=1}^{n_N} \int_{t_{i-1}}^{t_i} [\ldots] \mathrm{d}t \tag{36}$$

and $t_0 < t_1 < \ldots < t_{n_t} = t_0 + t_T$. Each $t \in I_n = [t_{n-1}, t_n]$ can be transformed to $\tau \in I_\tau = [0, 1]$ via the mapping

$$\tau(t) = \frac{t - t_{n-1}}{t_n - t_{n-1}}. \tag{37}$$

The trial functions $\boldsymbol{\alpha}(\tau)$ and $\boldsymbol{T}(\tau)$ are approximated on each subinterval I_n by smooth Lagrange polynomials of degree k

$$\boldsymbol{\alpha}^h(\tau)|_{I_n} = \sum_{i=1}^{k+1} M_i(\tau) \boldsymbol{\alpha}^i \quad \boldsymbol{T}^h(\tau)|_{I_n} = \sum_{i=1}^{k+1} M_i(\tau) \boldsymbol{T}^i \tag{38}$$

which are discontinuous across the element boundaries and given by

$$M_i(\tau) = \prod_{j=1; j \neq i}^{k+1} \frac{\tau - \tau_j}{\tau_i - \tau_j}, \qquad 1 \leq i \leq k+1. \tag{39}$$

The time derivatives take the format

$$\dot{\boldsymbol{T}}^h(\tau)|_{I_n} = \frac{1}{h_n} \sum_{i=1}^{k+1} M_i'(\tau) \boldsymbol{T}^i, \tag{40}$$

with $h_n = [t_n - t_{n-1}]$ being the length of the interval.

The test functions $\delta\boldsymbol{\alpha}$ and $\delta\boldsymbol{T}$ are elements of the same space as the trial functions such that they take the form

$$\delta\boldsymbol{\alpha}^h(\tau)|_{I_n} = \sum_{i=1}^{k+1} M_i(\tau) \delta\boldsymbol{\alpha}^i \quad \delta\boldsymbol{T}^h(\tau)|_{I_n} = \sum_{i=1}^{k+1} M_i(\tau) \delta\boldsymbol{T}^i. \tag{41}$$

A jump, thus a discontinuity, in the master element I_τ has to be admitted in order to prevent that the trial functions are over-determined at the nodal values, see Fig. 1.

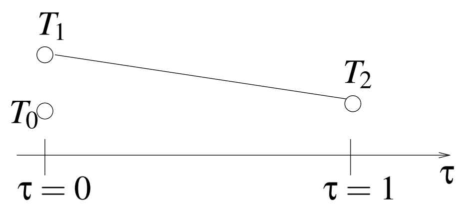

Figure 1 : The continuity condition is relaxed. Therefore one generally gets a jump $[\boldsymbol{T}^h]_0 = \boldsymbol{T}_1 - \boldsymbol{T}_0$. Here the discontinuity on the linear master element I_τ is shown

$[\boldsymbol{T}^h]_0 = \boldsymbol{T}_1 - \boldsymbol{T}_0$ denotes the amount of the jump at $\tau = 0$. $\boldsymbol{T}_0$ is the known value at the local node $\tau = 0$ from the previous time step.

The starting point of the time finite element method is, like in the space finite element method, the weak form. We now formulate the dG(k) approximation for heat flow of the Fourier type:

find a trial function $\boldsymbol{T}(t)$ such that

$$\int_0^1 \delta\boldsymbol{T}\left[\boldsymbol{C}_{\rho c}\dot{\boldsymbol{T}} + \boldsymbol{K}_k\boldsymbol{T} - \boldsymbol{F}_{\text{source}} + \boldsymbol{F}_I\right]\mathrm{d}\tau + \delta\boldsymbol{T}_1\left[\boldsymbol{T}^h\right]_0 = 0, \tag{42}$$

for all test functions $\delta\boldsymbol{T}$.

Taking into account the finite element approximations (38) and (41), we obtain the following set of algebraic equations:

$$\sum_{j=1}^{k+1}\int_0^1 M_i\boldsymbol{C}_{\rho c}M_j'\mathrm{d}\tau\boldsymbol{T}^j + h_n\int_0^1 M_i\boldsymbol{K}_kM_j\mathrm{d}\tau\boldsymbol{T}^j + h_n\delta_{i1}\left[\boldsymbol{T}^h\right]_0 = h_n\sum_{j=1}^{k+1}\int_0^1 M_i\left[\boldsymbol{F}_{\text{source}} - \boldsymbol{F}_I\right]\mathrm{d}\tau \tag{43}$$

for all $i = 1,\ldots,k+1$, where we introduced the Kronecker Delta δ_{i1}.

The discontinuous Galerkin and the finite element approximation of type II read

$$\int_0^1 \delta\boldsymbol{T}\left[\boldsymbol{C}_{\rho cb}\dot{\boldsymbol{T}} + \boldsymbol{K}_{\rho\frac{a}{b}k}\boldsymbol{\alpha} - \boldsymbol{F}_{\text{source}} + \boldsymbol{F}_{II}\right]\mathrm{d}\tau + \delta\boldsymbol{T}_1\left[\boldsymbol{T}^h\right]_0 = 0 \tag{44}$$

resp.

$$\sum_{j=1}^{k+1}\int_0^1 M_i\boldsymbol{C}_{\rho cb}M_j'\mathrm{d}\tau\boldsymbol{T}^j + h_n\int_0^1 M_i\boldsymbol{K}_{\rho\frac{a}{b}k}M_j\mathrm{d}\tau\boldsymbol{\alpha}^j + h_n\delta_{i1}\left[\boldsymbol{T}^h\right]_0 = h_n\sum_{j=1}^{k+1}\int_0^1 M_i\left[\boldsymbol{F}_{\text{source}} - \boldsymbol{F}_{II}\right]\mathrm{d}\tau \quad \forall i = 1,\ldots,k+1 \tag{45}$$

whereas those of type III are given by

$$\int_0^1 \delta\boldsymbol{T}\left[\boldsymbol{C}_{\rho\frac{a}{b}b_2}\dot{\boldsymbol{\alpha}} + \boldsymbol{C}_{\rho\frac{a}{b}b_3}\dot{\boldsymbol{T}} + \boldsymbol{K}_{k_1}\boldsymbol{\alpha} + \boldsymbol{K}_{k_2}\boldsymbol{T} - \boldsymbol{F}_{\text{s}} + \boldsymbol{F}_{III}\right]\mathrm{d}\tau + \delta\boldsymbol{T}_1\left[\boldsymbol{T}^h\right]_0 = 0 \tag{46}$$

resp.

$$\sum_{j=1}^{k+1}\int_0^1 M_i\boldsymbol{C}_{\rho\frac{a}{b}b_2}M_j'\mathrm{d}\tau\boldsymbol{\alpha}^j + \int_0^1 M_i\boldsymbol{C}_{\rho\frac{a}{b}b_3}M_j'\mathrm{d}\tau\boldsymbol{T}^j + h_n\int_0^1 M_i\boldsymbol{K}_{k_1}M_j\mathrm{d}\tau\boldsymbol{\alpha}^j + h_n\int_0^1 M_i\boldsymbol{K}_{k_2}M_j\mathrm{d}\tau\boldsymbol{T}^j + h_n\delta_{i1}\left[\boldsymbol{T}^h\right]_0 = h_n\sum_{j=1}^{k+1}\int_0^1 M_i\left[\boldsymbol{F}_{\text{source}} - \boldsymbol{F}_{III}\right]\mathrm{d}\tau \quad \forall i = 1,\ldots,k+1. \tag{47}$$

As we discretize $\boldsymbol{\alpha}$ as well as $\boldsymbol{T}$ the relation between $\boldsymbol{\alpha}$ and $\boldsymbol{T}$ has to be discretized, too. The weak form of (3)

$$h_n\int_0^1 \delta\boldsymbol{\alpha}\left[\dot{\boldsymbol{\alpha}} - \boldsymbol{T}\right]\mathrm{d}\tau + \delta\boldsymbol{\alpha}_1\left[\boldsymbol{\alpha}^h\right]_0 = 0 \tag{48}$$

leads to the discrete system

$$\sum_{j=1}^{k+1}\int_0^1 M_iM_j'\mathrm{d}\tau\boldsymbol{\alpha}^j - h_n\int_0^1 M_iM_j\mathrm{d}\tau\boldsymbol{T}^j + h_n\delta_{i1}\left[\boldsymbol{\alpha}^h\right]_0 = 0 \quad \forall i = 1,\ldots,k+1. \tag{49}$$

3.2.2 Continuous Galerkin Method

The cG(k) method uses trial functions consisting of continuous piecewise polynomials of degree k and test functions consisting of discontinuous piecewise polynomials of degree $k-1$. Therefore the number of algebraic equation is decreased by one in comparison to the dG method.

The trial functions $\boldsymbol{\alpha}(\tau)$ and $\boldsymbol{T}(\tau)$ are again approximated by

$$\boldsymbol{\alpha}^h(\tau)|_{I_n} = \sum_{i=1}^{k+1} M_i(\tau)\boldsymbol{\alpha}^i \quad \boldsymbol{T}^h(\tau)|_{I_n} = \sum_{i=1}^{k+1} M_i(\tau)\boldsymbol{T}^i \tag{50}$$

which this time are continuous across the element boundaries. The nodal shape functions of the test functions $\delta\boldsymbol{\alpha}_*$ and $\delta\boldsymbol{T}_*$ are of reduced degree $k-1$ such that $\delta\boldsymbol{\alpha}_*^h$ and $\delta\boldsymbol{T}_*^h$ are of the following format

$$\delta\boldsymbol{\alpha}^h(\tau)|_{I_n} = \sum_{i=1}^{k} \tilde{M}_i \delta\boldsymbol{\alpha}_*^i \qquad \delta\boldsymbol{T}^h(\tau)|_{I_n} = \sum_{i=1}^{k} \tilde{M}_i \delta\boldsymbol{T}_*^i. \tag{51}$$

The reduced nodal shape functions $\tilde{M}_i$ are defined by the relation

$$\dot{\boldsymbol{\alpha}}^h(\tau) = \frac{1}{h_n}\sum_{i=1}^{k+1} M_i'(\tau)\boldsymbol{\alpha}^i = \frac{1}{h_n}\sum_{i=1}^{k} \tilde{M}_i(\tau)\tilde{\boldsymbol{\alpha}}^i, \tag{52}$$

where the $\tilde{\boldsymbol{\alpha}}^i$s are linear combinations of the α^is (see also Tab. 1).

The cG(k) approximation of heat flow of type I is given by

$$h_n\int_0^1 \delta\boldsymbol{T}\left[\boldsymbol{C}_{\rho c}\dot{\boldsymbol{T}} + \boldsymbol{K}_k\boldsymbol{T} - \boldsymbol{F}_{\text{source}} + \boldsymbol{F}_I\right]\mathrm{d}\tau = 0, \tag{53}$$

the one of type II by

$$h_n\int_0^1 \delta\boldsymbol{T}\left[\boldsymbol{C}_{\rho cb}\dot{\boldsymbol{T}} + \boldsymbol{K}_{\rho\frac{a}{b}k}\boldsymbol{\alpha} - \boldsymbol{F}_{\text{source}} + \boldsymbol{F}_{II}\right]\mathrm{d}\tau = 0 \tag{54}$$

and the one of heat flow of type III yields

$$\begin{aligned} h_n\int_0^1 \delta\boldsymbol{T}[\boldsymbol{C}_{\rho\frac{a}{b}b_2}\dot{\boldsymbol{\alpha}} + \boldsymbol{C}_{\rho\frac{a}{b}b_3}\dot{\boldsymbol{T}} + \boldsymbol{K}_{k_1}\boldsymbol{\alpha} + \boldsymbol{K}_{k_2}\boldsymbol{T} \\ -\boldsymbol{F}_{\text{source}} + \boldsymbol{F}_{III}]\mathrm{d}\tau = 0. \end{aligned} \tag{55}$$

The relation (3) between $\boldsymbol{\alpha}$ and $\boldsymbol{T}$ follows:

$$h_n\int_0^1 \delta\boldsymbol{\alpha}[\dot{\boldsymbol{\alpha}} - \boldsymbol{T}]\mathrm{d}\tau = 0. \tag{56}$$

Regarding the arbitrariness of the test functions and inserting the relations (50), (51) and (52) into the weak form (54) of the temperature equation leads to the listed system of equations for type I:

$$\begin{aligned} &\sum_{j=1}^{k+1}\int_0^1 \tilde{M}_i\boldsymbol{C}_{\rho c}M_j'\mathrm{d}\tau\boldsymbol{T}^j + h_n\int_0^1 \tilde{M}_i\boldsymbol{K}_kM_j\mathrm{d}\tau\boldsymbol{T}^j \\ &= h_n\sum_{j=1}^{k+1}\int_0^1 \tilde{M}_i[\boldsymbol{F}_{\text{source}} - \boldsymbol{F}_I]\mathrm{d}\tau \quad \forall i = 1,\dots,k. \end{aligned} \tag{57}$$

Table 1 : Nodal shape functions $M_i(\tau)$ and $\tilde{M}_i(\tau)$ for polynomial approximations of degrees $k = 1, 2, 3$ along with associated values $\tilde{\alpha}^i$

	$M_i(\tau)$	$\tilde{M}_i(\tau)$	$\tilde{\alpha}^i$
$k=1$	$M_1 = 1-\tau$	$\tilde{M}_1 = 1$	$\tilde{\alpha}_1 = \alpha_2 - \alpha_1$
	$M_2 = \tau$		
$k=2$	$M_1 = [2\tau-1][\tau-1]$	$\tilde{M}_1 = 1-\tau$	$\tilde{\alpha}_1 = -3\alpha_1 + 4\alpha_2 - \alpha_3$
	$M_2 = -4[\tau^2-\tau]$	$\tilde{M}_2 = \tau$	$\tilde{\alpha} = \alpha_1 - 4\alpha_2 + 3\alpha_3$
	$M_3 = [2\tau-1]\tau$		
$k=3$	$M_1 = -\frac{9}{2}[\tau-\frac{1}{3}][\tau-\frac{2}{3}][\tau-1]$	$\tilde{M}_1 = [2\tau-1][\tau-1]$	$\tilde{\alpha}_1 = -\frac{11}{2}\alpha_1 + 9\alpha_2 - \frac{9}{2}\alpha_3 + \alpha_4$
	$M_2 = \frac{27}{2}[\tau-\frac{2}{3}][\tau-1]\tau$	$\tilde{M}_2 = -4[\tau^2-\tau]$	$\tilde{\alpha}_2 = \frac{1}{8}\alpha_1 - \frac{27}{8}\alpha_2 + \frac{27}{8}\alpha_3 - \frac{1}{8}\alpha_4$
	$M_3 = -\frac{27}{2}[\tau-\frac{1}{3}][\tau-1]\tau$	$\tilde{M}_3 = [2\tau-1]\tau$	$\tilde{\alpha}_3 = -\alpha_1 + \frac{9}{2}\alpha_3 + \frac{11}{2}\alpha_4$

Analogously, we receive the algebraic set of equations for type II

$$\sum_{j=1}^{k+1}\int_0^1 \tilde{M}_i \boldsymbol{C}_{\rho c b} M'_j \mathrm{d}\tau \boldsymbol{T}^j + h_n \int_0^1 \tilde{M}_i \boldsymbol{K}_{\rho \frac{a}{b} k} M_j \mathrm{d}\tau \boldsymbol{\alpha}^j = h_n \sum_{j=1}^{k+1}\int_0^1 \tilde{M}_i \left[\boldsymbol{F}_{\text{source}} - \boldsymbol{F}_{II}\right] \mathrm{d}\tau \quad \forall i = 1,\ldots,k \tag{58}$$

and type III:

$$\sum_{j=1}^{k+1}\int_0^1 \tilde{M}_i \boldsymbol{C}_{\rho \frac{a}{b} b_2} M'_j \mathrm{d}\tau \boldsymbol{\alpha}^j + \int_0^1 \tilde{M}_i \boldsymbol{C}_{\rho \frac{a}{b} b_3} M'_j \mathrm{d}\tau \boldsymbol{T}^j + h_n \int_0^1 \tilde{M}_i \boldsymbol{K}_{k_1} M_j \mathrm{d}\tau \boldsymbol{\alpha}^j + h_n \int_0^1 \tilde{M}_i \boldsymbol{K}_{k_2} M_j \mathrm{d}\tau \boldsymbol{T}^j = h_n \sum_{j=1}^{k+1}\int_0^1 \tilde{M}_i \left[\boldsymbol{F}_{\text{source}} - \boldsymbol{F}_{III}\right] \mathrm{d}\tau \quad \forall i = 1,\ldots,k. \tag{59}$$

In order to obtain a well-defined set of algebraic equations for both types of heat conduction equation (56) has to be discretized as well:

$$\sum_{j=1}^{k+1}\int_0^1 \tilde{M}_i M'_j \mathrm{d}\tau \boldsymbol{\alpha}^j - h_n \int_0^1 \tilde{M}_i M_j \mathrm{d}\tau \boldsymbol{T}^j = 0. \tag{60}$$

Table 2 : heat conduction problem: computational algorithm for one typical time step

Given:	initial conditions: $\boldsymbol{\alpha}, \boldsymbol{T}$ at time n time step size: h_n set time iteration number = n
Find:	$\boldsymbol{\alpha}, \boldsymbol{T}$ at time $n+1$
(1)	spatial discretization: compute $\boldsymbol{C}_\bullet, \boldsymbol{K}_\bullet, \boldsymbol{F}_{\text{source}}, \boldsymbol{F}_I, \boldsymbol{F}_{II}, \boldsymbol{F}_{III}$
(2)	temporal discretization: compute time integrals for $n+1$ $\int_0^1 \tilde{M}_i \boldsymbol{C}_\bullet M'_j \mathrm{d}\tau$, $\int_0^1 \tilde{M}_i M_j \mathrm{d}\tau$, $\int_0^1 \tilde{M}_i M'_j \mathrm{d}\tau$, ...
(3)	build algebraic system of equations $\boldsymbol{H}\begin{pmatrix}\boldsymbol{T}\\ \boldsymbol{\alpha}\end{pmatrix} = \begin{pmatrix}\boldsymbol{F}_{\text{eq1}}\\ \boldsymbol{F}_{\text{eq2}}\end{pmatrix}$ $\boldsymbol{H}$: matrix consisting of corresponding time integrals eq1: (43), (58) or (59) eq2: (60)
(4)	solve algebraic system of equations $\begin{pmatrix}\boldsymbol{T}\\ \boldsymbol{\alpha}\end{pmatrix} = \boldsymbol{H}^{-1}\begin{pmatrix}\boldsymbol{F}_{\text{eq1}}\\ \boldsymbol{F}_{\text{eq2}}\end{pmatrix}$

4 Numerical Example

In this section we present a numerical example in order to demonstrate the applicability of the proposed method. We study a rigid conductor of sodium fluoride (NaF) where the phenomenon of second sound was observed in a small temperature interval around 15K. An isotropic and homogeneous material is assumed and the material parameters were taken from Gmelin (1993). We apply the derived system of equations to a 1D-NaF-bar at 15K with a length of $l = 8.3$ mm.

$$\begin{aligned} &\rho = 2866\left[\frac{kg}{m^3}\right] && c = 2.774\left[\frac{W}{kgK}\right] \\ &k = 20500\left[\frac{W}{mK}\right] && k_1 = 20500\left[\frac{W}{mK}\right] \\ &k_2 = \frac{k_1}{10000}\left[\frac{W}{mK}\right] && l = 8.3\,[mm] \\ &r = 0 - \text{no external heat source} \end{aligned} \tag{61}$$

Initially the bar is set at equilibrium. Then we raise the temperature at the left side of the specimen by a short heat impulse with a height of $1.0K$. The thermal displacement $\boldsymbol{\alpha}$ is chosen to be equal to 0 on the entire bar.The observation time is $6\mu s$. We chose 200 finite elements in space and 80 in time in each of the examples.

4.1 Type I

Fig. 2 shows the temperature distribution according to Fourier's law generated by the dG(1)-method. The temperature is plotted as a function of space and time. It can be seen that the heat does not propagate as a wave.

In order to solve parabolic initial value problems the discontinuous Galerkin method gives bettter stability properties than the continuous Galerkin method [Eriksson, Estep, Hansbo, and Johnson (1996)]. In case of the parabolic Fourier temperature equation the cG-method does not lead to a reasonable solution at all.

4.2 Type II

Hardy and Jaswal (1971) specify the velocity of second sound in NaF at 15K to $19.531 \cdot 10^{-4} \frac{m}{\mu s}$. We set the constant $a := \frac{1}{\rho}$ and therefore receive $b \approx 10^3$, using equation

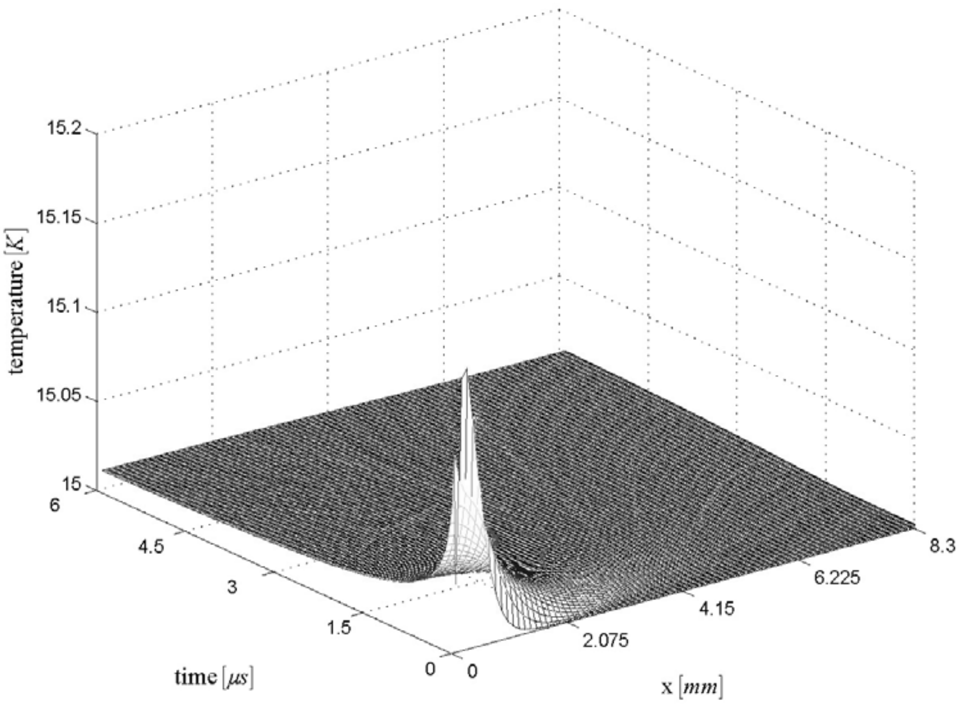

Figure 2 : Heat conduction in NaF, type I, dG approximation. Heat does not propagate as a wave.

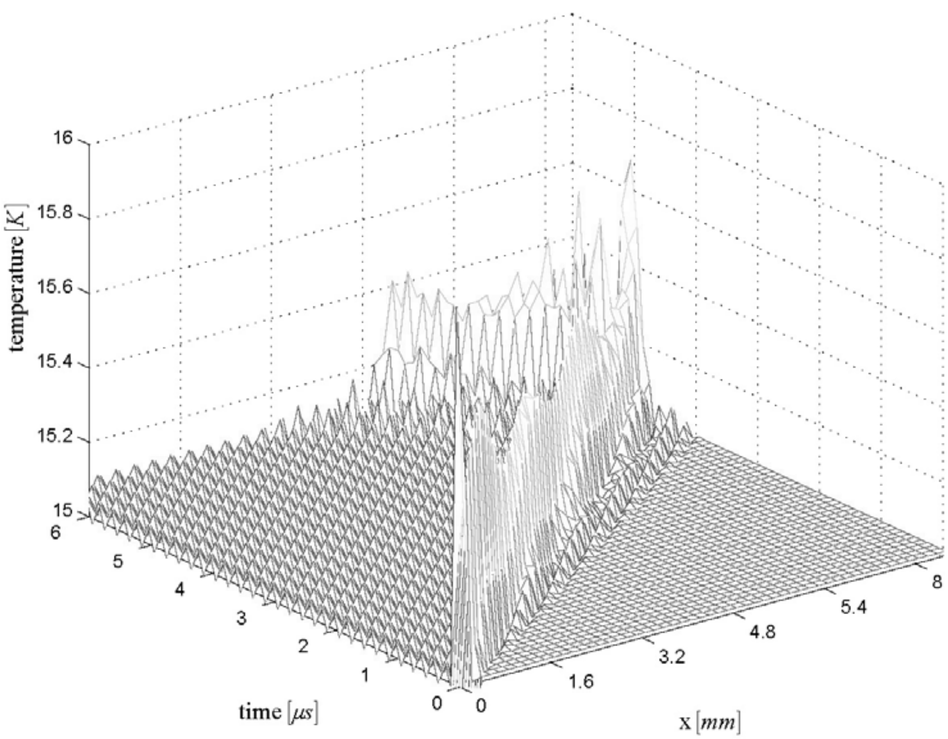

Figure 3 : Heat conduction in NaF, type II, cG approximation. Heat propagates as a wave. Oscillations enforce a stabilization.

(21). The heat flow of type II proves to be instable - a result which was also derived theoretically in the non-linear case by Quintanilla in Quintanilla (2001a). Fig. 3, which was generated by the cG-method, shows oscillations.

Thus we apply a Streamline-Upwind-Stabilization-Method, see also Appendix A. Fig. 4 shows the stabilized heat flow of type II.

A wave speed of $19.531 \cdot 10^{-5} \frac{m}{\mu s}$ is related to an arrival time of $4.1 \mu s$ in the considered specimen. The arrival point in this model is $4.25 \mu s$. As it has been mentioned before, heat flow of type II does not involve energy dissipation. As a consequence, the wave propagates endlessly between the two sides of the bar.

The dG approximation proves to be even more unstable. The quality of the solution depends too strongly on the intial conditions and the number of elements. For most tries a wrong solution is received. Although type II is originally a theory without energy dissipation, the dG approximation shows a slight diffusive behavior. This is due to the (numerical) damping properties of the dG method. The dG method is not energy conserving. Because of the discontinuous dG test functions the algebraic system to be solved has twice the size of the cG algebraic system.

Therefore the cG method seems to be the better choice for a theory without energy dissipation.

Fig. 5 shows heat conduction in NaF of type II generated by a dG method. The result is more stable than the cG approximation, but numerical oscillations can be seen in the beginning of the computation. We used 45 temporal and 50 spatial elements as the solution achieved with 200 temporal and 80 spatial elements was wrong.

4.3 Type III

In the case of heat flow of type III we set $a := c$, $b_2 = 0$ and $b_3 = 1$. Consequently, b must be equal to 10^{-6}. We used the same amount of elements as in the type II case (again 80 spatial and 200 temporal) and did not apply any stabilization method. Note that although $\frac{k_1}{k_2} = \frac{10000}{1}$ the method is stable. The arrival point is perfectly met. This heat conduction model involves dissipation. Thus the wave amplitude decreases and the wave becomes diffusive. Depending on the ratio $k_1 : k_2$ the model of type III is more or less diffusive. Even with the selected ratio of $10000 : 1$ the diffusion is clearly visible (see Fig. 6 and Fig. 7). Both, cG and dG, lead to a satisfactory solution. The amplitude of the dG approximation is slightly smaller than the one of the cG solution. This is due to numerical damping effects of the dG method.

We chose the length of the bar to be 8.3 mm in order to be able to compare our numerical results to those obtained by Cimmelli and Frischmuth with their approach in Cimmelli and Frischmuth (1996) and Frischmuth and Cimmelli (1996). We found a good correspondance with arrival times and the height of the heat impulse at the left end of the bar. Inbetween the amplitude differs due to the different theoretical models.

5 Conclusions

The objective of this paper was the investigation and comparison of heat conduction following the approach of Green and Naghdi. Motivated by the fully consistent theory and the basic general development, we began by reviewing their equations of non-classical heat conduction and then introduced discretization methods which are based on finite elements in space and in time. As predicted by Eriksson, Estep, Hansbo, and Johnson (1996) the dG method is better suited for parabolic problems whereas the cG methods works better for hyperbolic problems. It turned out that due to the instability of type II we had to use a Streamline-Upwind-Stabilization for this kind of heat flow. As Eriksson, Estep, Hansbo, and Johnson (1996) predictes, also in the case of heat propagation dG proves to be better suitable for the parabolic problem and cG better for the hyperbolic one.

As expected, Fourier's law is inapplicable to heat conduction in NaF at the considered temperature. Type II and III describe the behavior of second sound adequately. The heat propagates at finite speed and as waves. Our numerical results agree very well with experimental data (see Jackson and Walker (1970, 1971)) as well as with the numerical results of Cimmelli and Frischmuth (1996); Frischmuth and Cimmelli (1996). In contrast to other theories the approach of Green and Naghdi does not necessarily involve energy dissipation.

In our opinion their elegant theory is very promising and, agreeing with Green and Naghdi, "perhaps a more natural candidate for its identification as thermoelasticity" [Green and Naghdi (1993)]. In this paper the applicability to thermal problems of the theory was shown by means of a numerical example and the expected results were achieved.

Acknowledgement: The financial support by the Ger-

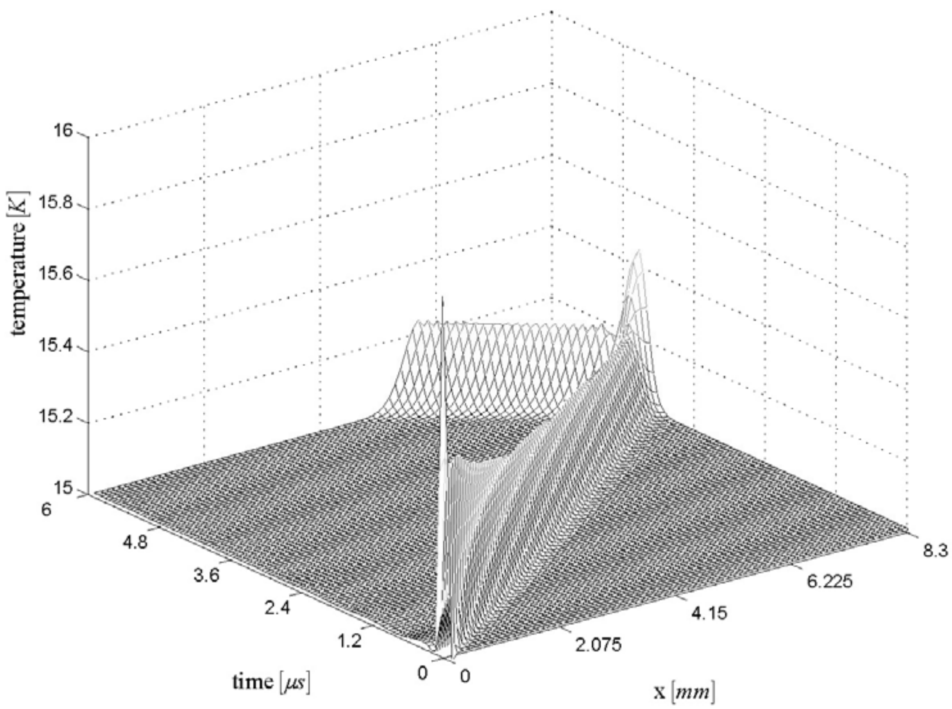

Figure 4 : Type II, approximated by cG and stabilized with a Streamline-Upwind-Method, does not involve energy dissipation.

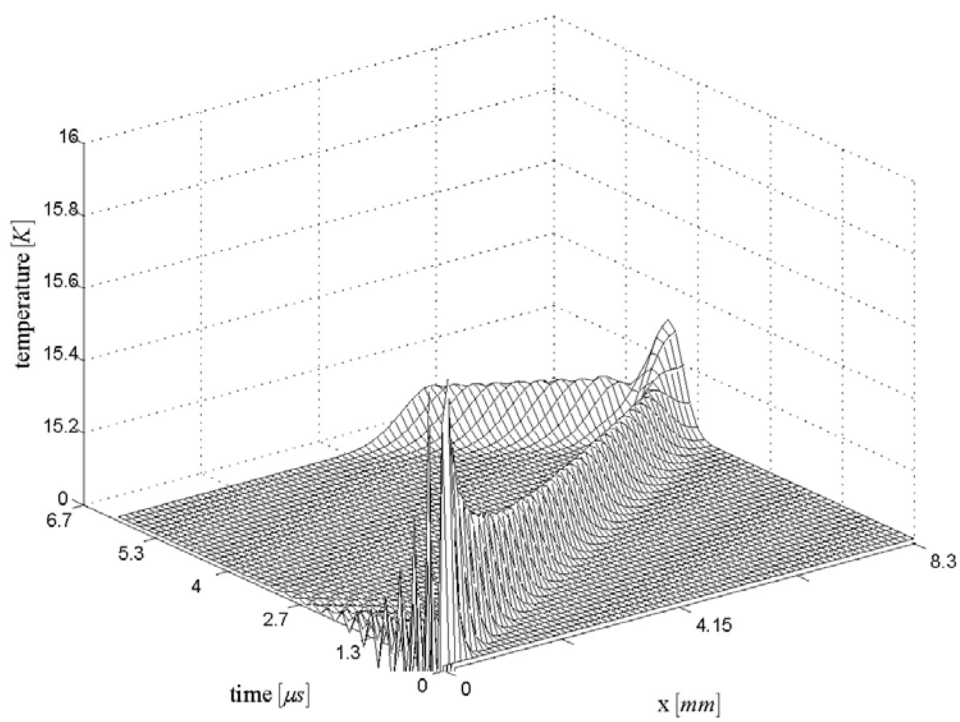

Figure 5 : Type II, approximated by dG, does involve small energy dissipation.

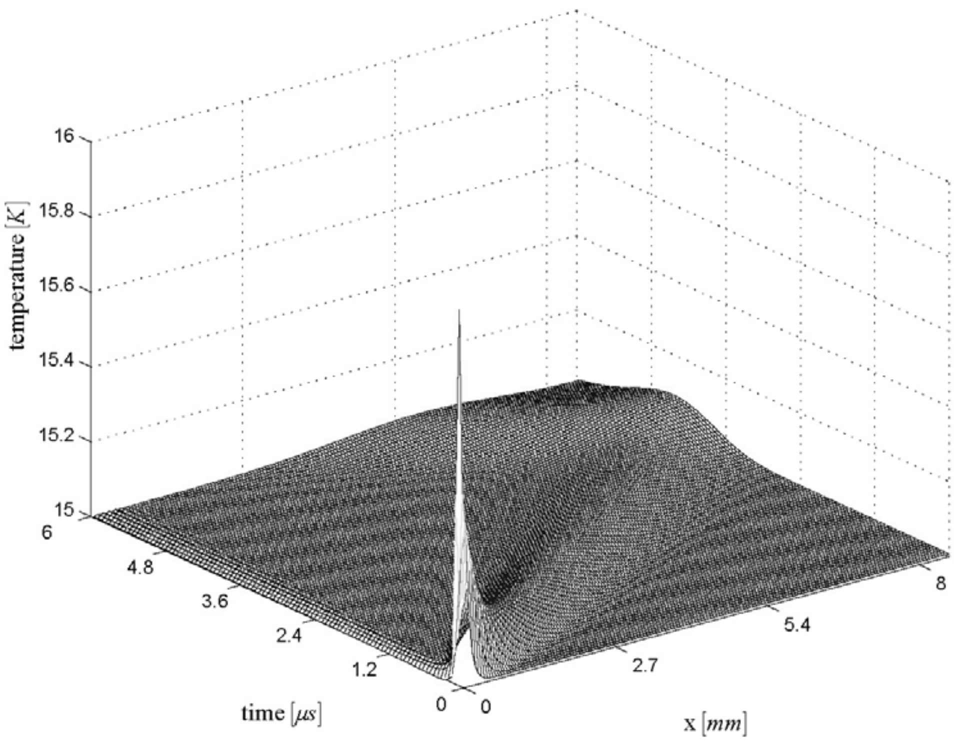

Figure 6 : Heat conduction in NaF, type III, cG approximation, permits propagation of heat as a diffusive wave. This heat flow is perfectly stable.

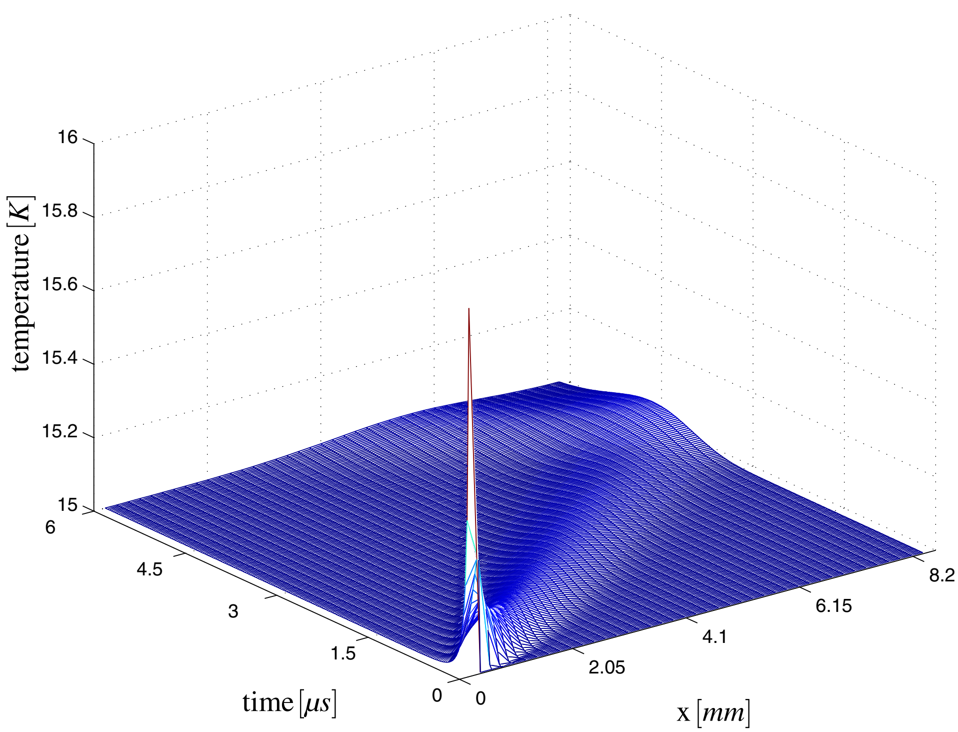

Figure 7 : Heat conduction in NaF, type III, dG approximation, permits propagation of heat as a diffusive wave. This heat flow is perfectly stable.

man Science Foundation (DFG) is gratefully acknowledged.

References

Ackermann, C.; Bertram, B.; Fairbank, H.; Gyuer, R. (1966): Second sound in solid helium. *Phys. Rev.*, vol. 16, no. 18, pp. 789–791.

Allam, M.; Elsibai, K.; AbouElregal, A. (2002): Thermal stresses in a harmonic field for an infinite body with a circular cylindrical hole without energy dissipation. *J. Thermal Stresses*, vol. 25, no. 1, pp. 57–67.

Betsch, P.; Steinmann, P. (2000): Conservation properties of a time fe method. part I: time -stepping schemes for n-body problems. *Int. J. Num. Meth. Eng.*, vol. 49, pp. 599–638.

Betsch, P.; Steinmann, P. (2000): Inherently energy conserving time finite elements for classical mechanics. *J. Comp. Phys.*, vol. 160, pp. 88–116.

Betsch, P.; Steinmann, P. (2001): Conservation properties of a time fe method - part II: time-stepping schemes for non-linear elastodynamics. *Int. J. Num. Meth. Eng.*, vol. 50, pp. 1931–1955.

Chandrasekharaiah, D. (1996): A note on the uniqueness of solution in the linear theory of thermoelasticity without energy dissipation. *J. Elasticity*, vol. 43, pp. 279–283.

Chandrasekharaiah, D. (1996): One-dimensional wave propagation in the linear theory of thermoelasticity without energy dissipation. *J. Thermal Stresses*, vol. 19, pp. 695–710.

Chandrasekharaiah, D. (1998): Hyperbolic thermoelasticity: A review of recent literature. *Appl. Mech. Rev.*, vol. 51, no. 12, pp. 705–729.

Cimmelli, V.; Frischmuth, K. (1996): Hyperbolic heat conduction at cryogenic temperatures. *Rendiconti del Circolo Matematico di Palermo*, vol. 45, pp. 137–145.

Cimmelli, V.; Kosiński, W. (1991): Nonequilibrium semi-empirical temperature in materials with thermal relaxation. *Arch. Mech.*, vol. 43, no. 6, pp. 753–767.

Eriksson, K.; Estep, D.; Hansbo, P.; Johnson, C. (1996): *Computational differential equations*. Studentlitteratur.

Frischmuth, K.; Cimmelli, V. (1996): Hyperbolic heat conduction with variable relaxation time. *J. Theor. Appl. Mech.*, vol. 34, no. 1, pp. 58–65.

Gmelin, L. (1993): *Gmelin handbook of inorganic and organometallic chemistry*. Springer.

Green, A.; Naghdi, P. (1977): On thermodynamics and the nature of the second law. In *Proc. R. Soc. Lond. 357*, pp. 253–270.

Green, A.; Naghdi, P. (1991): A re-examination of the basic postulates of thermomechanics. In *Proc. R. Soc. Lond. 432*, pp. 171–194.

Green, A.; Naghdi, P. (1992): On undamped heat waves in an elastic solid. *J. Thermal Stresses*, vol. 15, pp. 253–264.

Green, A.; Naghdi, P. (1993): Thermoelasticity without energy dissipation. *J. Elasticity*, vol. 31, pp. 189–208.

Hardy, R.; Jaswal, S. (1971): Velocity of second sound in naf. *Phys. Rev. B*, vol. 3, no. 12, pp. 4385–4387.

Hetnarski, R.; Ignaczak, J. (1996): Soliton-like waves in a low-temperature non-linear solid. *Int. J. Eng. Sci.*, vol. 34, pp. 1767–1787.

Hulme, B. (1972): One-step piecewise polynomial galerkin methods for initial value problems. *Math. Comput.*, vol. 26, no. 118, pp. 415–426.

Iesan, D. (1998): On the theory of thermoelasticity without energy dissipation. *J. Thermal Stresses*, vol. 21, pp. 295–307.

Jackson, H.; Walker, C. (1970): Second sound in NaF. *Phys. Rev.*, vol. 25, no. 1, pp. 26–28.

Jackson, H.; Walker, C. (1971): Thermal conductivity, second sound, and phonon-phonon interactions in NaF. *Phys. Rev. B*, vol. 3, no. 4, pp. 1428–1439.

Joseph, D.; Preziosi, L. (1989): Heat waves. *Rev. Mod. Phys.*, vol. 61, no. 1, pp. 41–73.

Joseph, D.; Preziosi, L. (1990): Addendum to the paper "heat waves". *Rev. Mod. Phys.*, vol. 62, no. 2, pp. 375–391.

Lasaint, P.; Raviart, P. (1974): *Mathematical Aspects of Finite Elements in Partial Differential Equations*, chapter On a finite element method for solving the neutron transport equation, pp. 89–123. Academic Press: New York, 1974.

Maugin, G.; Kalpadikes, V. (2002): A hamiltonian formulation for elasticity and thermoelasticity. *J. Phys. A: Math. Gen.*, vol. 35, pp. 10775–10788.

Maugin, G.; Kalpadikes, V. (2002): The slow march towards an analytical mechanics of dissipative materials. *Technische Mechanik*, vol. 22, no. 2, pp. 98–103.

Misra, J.; Chattopadhyay, N.; Chakravorty, A. (2000): Study of thermoelastic wave propagation in a half-space using GN theory. *J. Thermal Stresses*, vol. 23, pp. 327–351.

Nappa, L. (1998): Spatial decay estimates for the evolution equations of linear thermoelasticity withouth energy dissipation. *J. Thermal Stresses*, vol. 21, pp. 581–592.

Peshkov, V. (1944): *J. Phys. USSR*, vol. 8, pp. 831.

Peshkov, V. (1946): *Inter. Conf. Fund. Particles and Low Temperatures: Report*, vol. Cambridge, July 22-27.

Puri, P.; Jordan, P. (2004): On the propagation of plane waves in type-III thermoelastic media. *Proc. R. Soc. Lond. A*, vol. 460, pp. 3203–3221.

Quintanilla, R. (2001): Instability and non-existence in the nonlinear theory of thermoelasticity without energy dissipation. *Continuum Mech. Thermodyn.*, vol. 13, pp. 121–129.

Quintanilla, R. (2001): Structural stability and continuous dependence of solutions of thermoelasticity of type III. *Discrete and Continuous Dynamical Systems-Series B*, vol. 1, no. 4, pp. 463–470.

Quintanilla, R. (2002): Existence in thermoelasticity without energy dissipation. *J.Thermal Stresses*, vol. 25, no. 2, pp. 195–202.

Quintanilla, R.; Straughan, B. (2004): A note on discontinuity waves in type III thermoelasticity. *Proc. R. Soc. Lond. A*, vol. 460, pp. 1169–1175.

Tamma, K.; Namburu, R. (1997): Computational approaches with applications to non-classical and classical thermomechanical problems. *Appl. Mech. Rev.*, vol. 60, no. 9, pp. 514–551.

Tzou, D. (1995): A unified approach for heat conduction from macro- to micro-scales. *ASME J. Heat Transfer*, vol. 117, pp. 8–16.

Appendix A: Stabilisation of type II

In case of heat conduction in NaF, type II, numerical errors cause oscillations. Therefore we apply a stabilization technique. The basic weak form of type II reads:

$$\int_I \int_B \delta T \left[\rho c b^2 \dot{T} - k \Delta \alpha\right] \mathrm{d}V \mathrm{d}t = 0 \tag{A1}$$

Most stabilization methods add a so-called stabilization term ST to the original equation:

$$\int_I \int_B \delta T \left[\rho c b^2 \dot{T} - k \Delta \alpha\right] \mathrm{d}V \mathrm{d}t + ST = 0 \tag{A2}$$

In the following we shortly introduce different stabiliation approaches. In all cases the main idea is a perturbation of the test function.
Streamline-Upwind-methods use test functions of the kind

$$\overline{\delta T} = \delta T + \varepsilon \boldsymbol{a} \nabla T, \tag{A3}$$

with ε being called the stabilization parameter and $\boldsymbol{a}$ being an arbitrary vector. Simple Streamline-Upwind-methods apply the perturbation only to one part of the equation (e.g. to the advection term of an advection-diffusion-equation). In our case, we receive:

$$ST = \varepsilon \boldsymbol{a} \int_I \int_B \nabla \delta T \rho c b^2 \dot{T} \mathrm{d}V \mathrm{d}t. \tag{A4}$$

Integrating by parts and neglecting the boundary terms, the heat equation modified by SU-stabilization reads:

$$\rho c b^2 \left[1 - \varepsilon \boldsymbol{a} \nabla\right] \dot{T} - k \Delta \alpha = 0. \tag{A5}$$

Choosing $\varepsilon = -5 \cdot 10^{-6}$ results in Fig. 4
Applying the pertubation to $-k\Delta\alpha$ leads to the stabilization term

$$ST = \varepsilon \boldsymbol{a} \int_I \int_B \nabla \delta T \left[-k \Delta \alpha\right] \mathrm{d}V \mathrm{d}t \tag{A6}$$

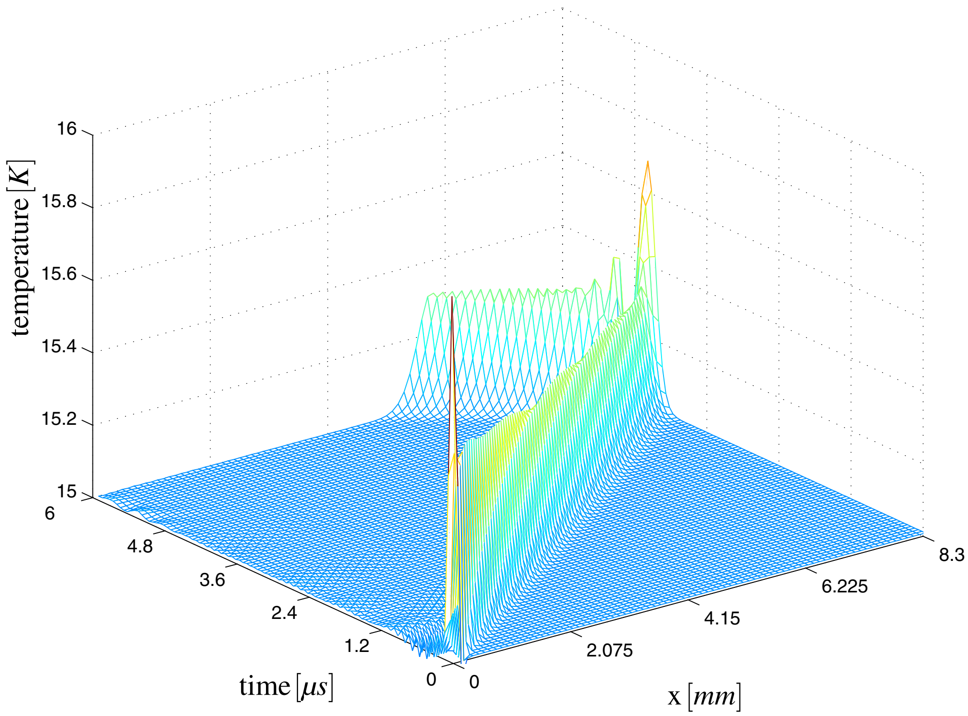

Figure 8 : Type II, stabilized with SUPG

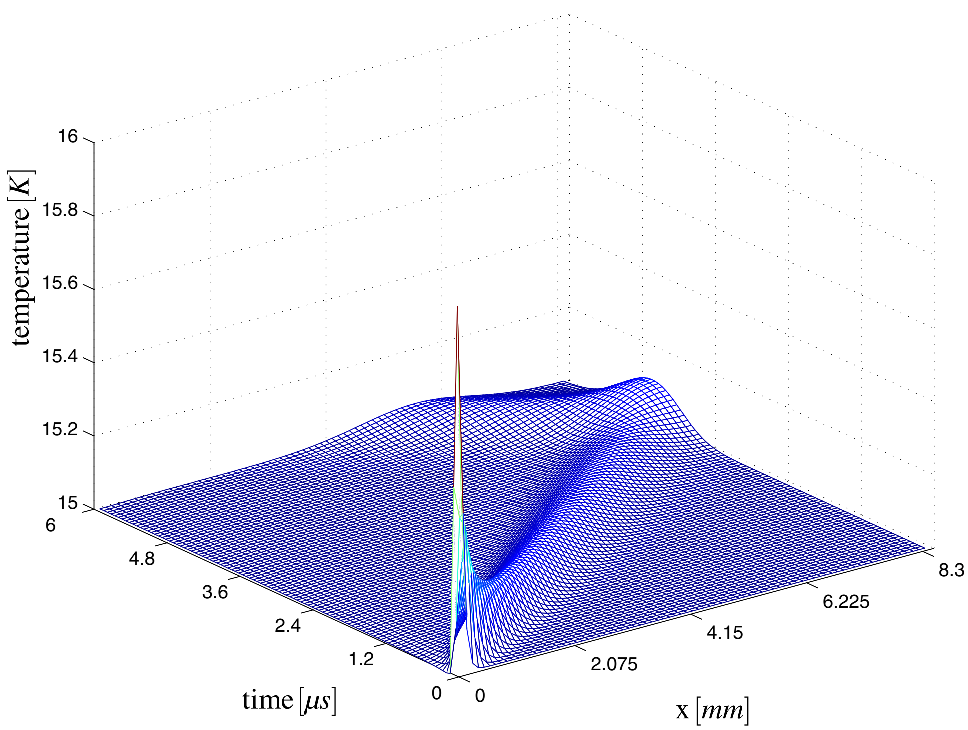

Figure 9 : Type II, stabilized in time

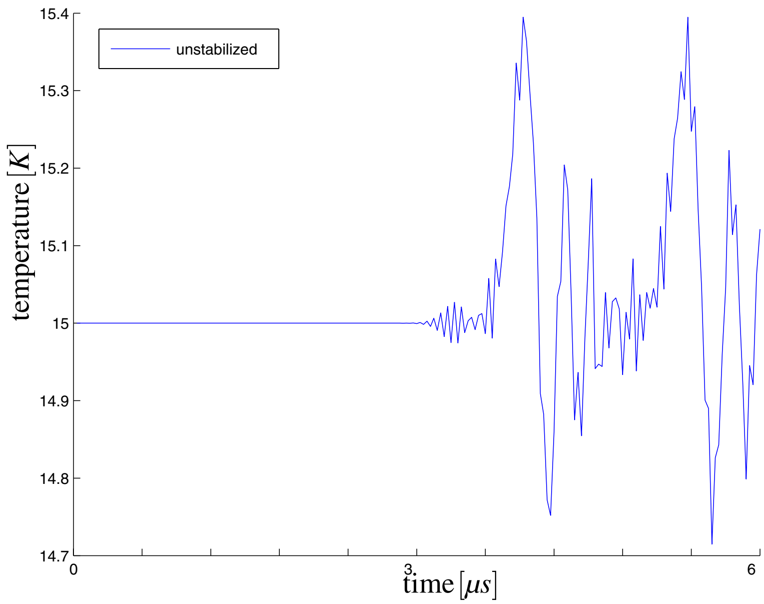

Figure 10 : Temperature is plotted versus time in the unstabilized case at x= 7mm. The oscillations of the solution are clearly visible.

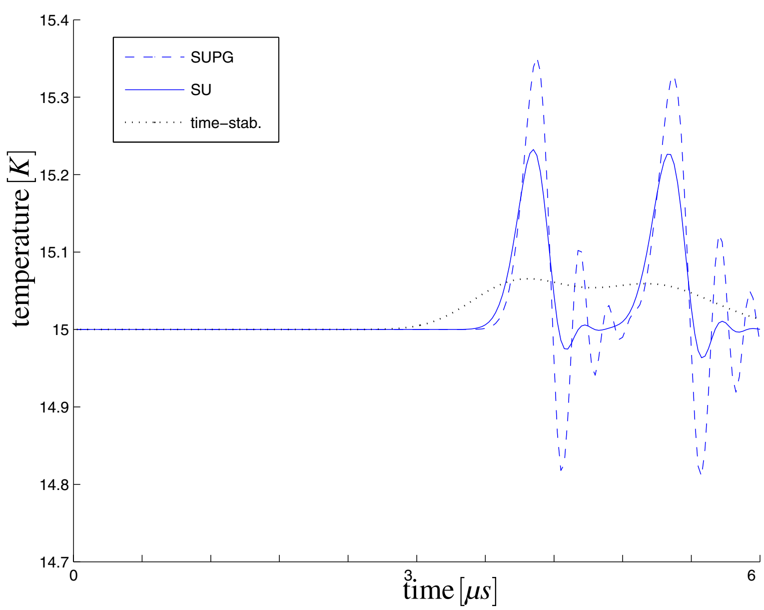

Figure 11 : Stabilized problem: Temperature is plotted versus time at x= 7mm. The SUPG-solution reveals diffusive characteristics: the amplitude of the original wave is larger than the reflected wave's one. Also it still contains oscillations. The SU-solution contains almost no dissipation and shows improved damping behavior. The time-stabilized solution does not seem to be appropriate since the solution is diffusive, amplitudes are damped too much and wave lengths become too large.

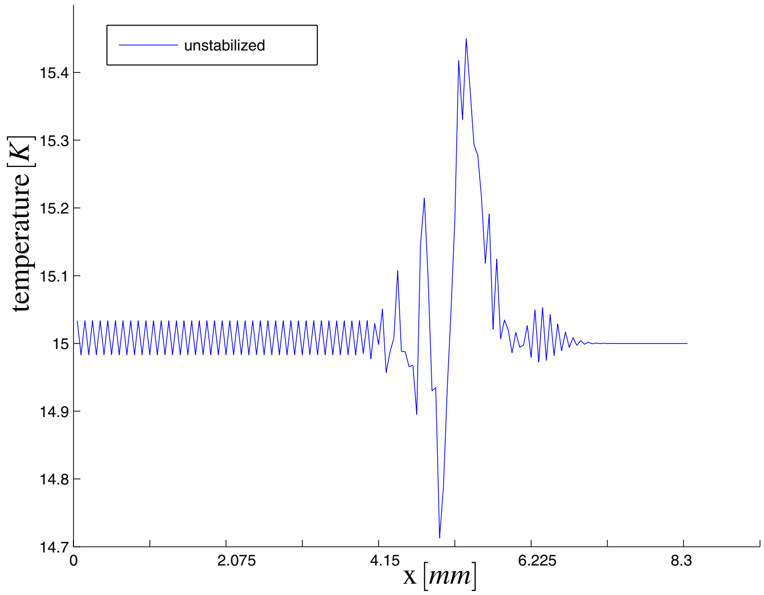

Figure 12 : Temperature is now plotted versus position in the unstabilized case at time $t = 3\mu$ s. Oscillations are again clearly visible.

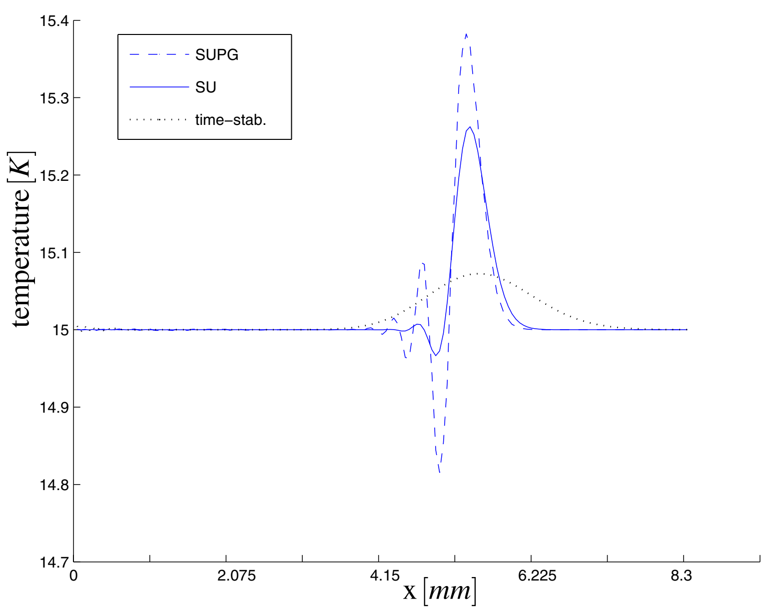

Figure 13 : Stabilized problem: Temperature plotted versus position at time $t = 3\mu$ s. Again it can be seen that the SUPG-solution oscillates and that the time-stabilized wave is damped too much whereas the SU-solution seems to be suitable.

resp. to the modified heat equation

$$\rho c b^2 \dot{T} - k\left[1 - \varepsilon \boldsymbol{a} \nabla\right] \Delta\alpha = 0 \tag{A7}$$

but not to a satisfactory solution.

An enlargement of the SU-method was developed by Hughes, the Streamline-Upwind/Petrov-Galerkin-method (SUPG). The test function (A3) is applied to the entire heat equation:

$$ST = \int_I \int_B \varepsilon \boldsymbol{a} \nabla \delta T \left[\rho c b^2 \dot{T} - k\Delta\alpha\right] \mathrm{d}V \mathrm{d}t \tag{A8}$$

After integrating by parts and neglecting the boundary terms, the heat equation modified by SUPG-stabilization reads:

$$\rho c b^2 \left[1 - \varepsilon \boldsymbol{a} \nabla\right] \dot{T} - k\left[1 - \varepsilon \boldsymbol{a} \nabla\right] \Delta\alpha = 0. \tag{A9}$$

Again we receive a stabilized heat flow:

The SUPG-stabilized heat flow (see Fig. 8) stills contains small numerical errors, e.g. the amplitude of the wave is slightly oscillating.

As the heat equation is transient the test function can be perturbated in time instead of in space as well:

$$\hat{\delta T} = \delta T + \varepsilon^\star \delta \dot{T}. \tag{A10}$$

If we apply this test function to $-k\Delta\alpha$, reflecting the spatial SU-method, we receive:

$$ST = \int_I \int_B \varepsilon^\star \delta \dot{T} \left[-k\Delta\alpha\right] \mathrm{d}V \mathrm{d}t = 0. \tag{A11}$$

It can be shown that for $\varepsilon = \frac{k_2}{k_1}$ equation (A2) is equivalent to heat flow of type III:

$$\rho c b^2 \dot{T} - k\left[1 - \varepsilon^\star \frac{\partial}{\partial t}\right] \Delta\alpha = 0. \tag{A12}$$

Consequently, we receive a heat flow which is dissipative although type II originally is not, see Fig. 9.

The two-dimensional plots of the temperature history, see Fig. 10 and Fig. 11, and those of temperature plotted versus place, see Fig. 12 and Fig. 13, show the numerical difficulties encountered and the effects of the different stabilization approaches. Fig. 10 and Fig. 12 demonstrate the oscillating cG-solution of type II heat flow. Fig. 11 and Fig. 13 reveal the behavior of SU, SUPG and time-stabilization whereas SU proves to be the most appropriate stabilization method.

Neither applying the perturbation to $\rho c b^2 \dot{T}$ nor applying (A10) to (A1), following the way of SUPG, leads to a reasonable solution. The stabilization terms read

$$ST = \int_I \int_B \varepsilon^\star \delta \dot{T} \rho c b^2 \dot{T} \mathrm{d}V \mathrm{d}t \tag{A13}$$

resp.

$$ST = \int_I \int_B \varepsilon^\star \delta \dot{T} \left[\rho c b^2 \dot{T} - k\Delta\alpha\right] \mathrm{d}V \mathrm{d}t \tag{A14}$$

whereas the modified heat equations

$$\rho c b^2 \left[1 - \varepsilon^\star \frac{\partial}{\partial t}\right] \dot{T} - k\Delta\alpha = 0 \tag{A15}$$

resp.

$$\rho c b^2 \left[1 - \varepsilon^\star \frac{\partial}{\partial t}\right] \dot{T} - k\left[1 - \varepsilon^\star \frac{\partial}{\partial t}\right] \Delta\alpha = 0 \tag{A16}$$

are to be solved.